Empirical Magnetic Field Models for the Space Weather Program

N. A. Tsyganenko [1]

NASA GSFC, Greenbelt, Maryland

A brief review is presented of the recent progress and the current state of the data-based modeling of the magnetospheric magnetic field. Combining the wealth of the observational data with flexible and realistic models advances our understanding of the dynamics of Earth's magnetic environment. The empirical approach to the modeling not only makes it possible to quantitatively represent the variable magnetosphere, but helps derive from data valuable information on its response to variations in interplanetary conditions. The cornerstones of the empirical modeling are (1) large sets of magnetic field and plasma data, (2) mathematical methods, allowing one to flexibly represent the B-field on a global scale, and (3) parameterization of magnetospheric field sources by the solar wind state variables and ground activity indices. This paper overviews most recent accomplishments made along these lines and discusses ongoing efforts to improve the data-based models; in particular, replicating the highly variable configuration of the magnetotail, introducing more flexible and realistic ring current model, and taking into account the variable shape and size of the magnetopause. Of special importance is the need to develop an improved representation of the high-latitude magnetosphere, including the dynamical large-scale Birkeland currents. Most of these problems can now be tackled, owing to recently devised powerful mathematical techniques, and a large amount of data obtained during several decades of spaceflight.

1. INTRODUCTION

The modeling of the global geomagnetic field has a unique place in space-weather studies. The magnetic field underlies all processes in the near-Earth environment: it links the interplanetary medium with the ionosphere, guides energetic charged particles, channels low-frequency electromagnetic waves, confines the radiation belts, directs electric currents, and stores huge amounts of energy, intermittently dissipated in the course of magnetospheric disturbances. If we know the field configuration, we can compare observations in different regions by mapping them along the magnetic field lines. Empirical models are needed to extract full information on the magnetospheric structure and its response to the solar wind conditions from observations. They serve as our main guide to magnetospheric structure, and their role has been justly compared to that of maps in the exploration of a new country.

Creating an empirical model involves three essentially different tasks. First, one needs to compile large sets of space magnetometer data and tag them by the concurrent information on the solar wind state and by suitable indices of the ground geomagnetic activity. Second, one has to develop flexible and physically sensible mathematical representation of the B-field on a global scale, in which contributions from individual field sources are given by separate terms. Third, a meaningful choice should be made of the input parameters, with which the amplitude and geometry of the principal

[1] Also at Raytheon Information, Technology, and Scientific Services (ITSS) Corporation, Lanham, Maryland.

Space Weather
Geophysical Monograph 125

magnetospheric current systems are to be related. Substantial progress has taken place recently along the above lines [*Tsyganenko*, 1995, 1998b, 2000b; *Ostapenko and Maltsev*, 1997]. Instead of a crude binning into several intervals of the ground activity levels, adopted in early work [*Mead and Fairfield*, 1975; *Tsyganenko and Usmanov*, 1982; *Tsyganenko*, 1987, 1989a] the latest model [*Tsyganenko,* 1996; referred below T96] features: (1) a continuous dependence on the solar wind pressure, Dst-index, and interplanetary magnetic field (IMF) components, (2) an explicitly defined magnetopause with realistic shape and size and controlled by the solar wind, (3) interconnection with the IMF, modeling the open magnetosphere, (4) Birkeland currents, parameterized by the solar wind pressure and IMF.

Significant further advance is expected with abundant data from new missions and recently developed new methods, with which we intend to model the observed polar cusp structure, the variable shape of the magnetopause, and a realistic ring current and magnetotail. After that, we still need better modeling of the high-latitude magnetosphere, including the dynamical large-scale Birkeland currents. These and other problems are briefly overviewed in this paper.

2. THREE "PILLARS" OF THE DATA-BASED MAGNETOSPHERE MODELING

Unlike the main geomagnetic field on the Earth's surface, the distant magnetic field varies constantly due to changing conditions in the solar wind and internal magnetospheric instabilities. Quantitative models should be able to replicate essential features of the response of the magnetospheric configuration to the variable external input. The magnetospheric response to the solar wind and IMF conditions is complicated by "memory" effects, so each measurement inside the magnetosphere should be provided with information not only on the current state of the interplanetary medium, but also with data of the preceding time interval, of an hour or more. Another input is ground-based information, in particular the geomagnetic indices. While the Kp- and AE-indices seem less suited for calibrating models, the Dst index, in spite of its drawbacks [*Campbell,* 1996], can serve as a good measure of the overall strength of the near-Earth electric currents, and its inclusion in parametric relations improves the agreement between observed and predicted fields [*Tsyganenko,* 1996, 2000a].

Magnetospheric and solar wind observations, complemented by concurrent ground-based data, are the first "pillar" of the data-based modeling. Over the past three decades, a vast amount of such data was collected by many spacecraft at different locations, seasons, solar cycle stages, and disturbance levels. *Mead and Fairfield* [1975] compiled the first set of distant magnetic field data, taken by four IMP spacecraft during 1966-1972, and used it to create an empirical model, binned by Kp-index. *Tsyganenko and Usmanov* [1982] added HEOS-1 and -2 data to the set of Mead and Fairfield and developed a more realistic model with an explicitly defined ring current and a tail current sheet. The dataset was further extended by Tsyganenko and Malkov [see *Peredo et al.,* 1993] who added ISEE 1/2 data from 1977-81, while Fairfield independently added HEOS observations and additional IMP-6 data to the original Mead-Fairfield data base. Editing of those data and merging them into one large database resulted in a set described by *Fairfield et al.* [1994]. It was used in the derivation of the T96 global field model, which not only represented average static configurations, but also revealed the response of individual field sources to changes in the external conditions.

As large as that dataset was, it became clear that much more data were needed, covering the full range of all variables – not only the {X,Y,Z} coordinates, but also the added dimensions of the geodipole tilt angle, the geomagnetic activity level (e.g., Dst-index), solar wind pressure, and IMF components. In this respect, the existing dataset still had many gaps. In particular, the great majority of the data came from quiet and moderately disturbed periods, while unusual conditions in the solar wind (most important for the space weather) were significantly underrepresented. The new observations during the last decade filled numerous gaps in the coverage. In particular, Geotail spacecraft provided excellent mapping of the tail plasma sheet, especially in its near-Earth part, where most interesting space weather phenomena take place. POLAR spacecraft, owing to its highly inclined orbit, greatly improved the sampling at high latitudes, including the polar cusps and the very important region of Birkeland currents. These new data made it possible to quantitatively study the variable structure of the tail current sheet and polar cusps, and stimulated the development of new modeling methods for representing all those features [e.g., *Tsyganenko et al.,* 1998; *Tsyganenko*, 1998, 2000b,c; *Tsyganenko and Russell,* 1999].

The second pillar of a magnetospheric model is its mathematical "frame." Close to Earth ($R \leq 6R_E$), the internal field dominates and its mathematical representation by spherical harmonics, established long ago by Gauss, is simple and straightforward. In contrast, the external part of the magnetic field is highly variable, non-potential, and has a complex structure, dictated by the magnetospheric plasma. Its relative contribution rapidly increases beyond $R \sim 6R_E$ and is dominant at $R \geq 8 - 10R_E$. Accurate, physically sensible, mathematically flexible, and reasonably simple representation of that part of the field is the major challenge.

The recent progress in that area is covered in part in earlier reviews [*Tsyganenko*, 1998b, 2000b]. In general, the approach is to represent the external field by a sum of modules, each representing an individual source, with its own geometry and its own response to external factors and the Earth's

dipole tilt. For example, the ring current residing in the inner magnetosphere varies relatively slowly and follows the orientation of the geodipole axis, while the magnetopause and the associated Chapman-Ferraro currents respond more rapidly to variations in the interplanetary medium, and their position is controlled mainly by the solar wind flow.

Modeling the magnetopause and its contribution to the total field has a special place in data-based modeling, since the confining effect of the boundary currents should take into account every source of the magnetospheric field and should also allow a controlled interconnection of the geomagnetic and interplanetary fields. The T96 model uses an analytical magnetopause, based on that of *Sibeck et al.* [1991], obtained by fitting an ellipsoid of revolution to a set of direct crossings. The distant tailward magnetopause in that model was represented by a cylinder, smoothly joining the ellipsoidal surface in the distant tail. *Shue et al.* [1997, 1998] suggested another approximation for the boundary and fitted it to a different set of crossings. Using the hemi-ellipsoidal magnetopause, however, has an important advantage: it allows a simple class of deformations, making it possible to easily reproduce a re-configuration of the cross-tail electric current without violating the shielding of the total field. It also allows one to replicate the realistic shape of the model magnetopause near the polar cusps as a simple modification of one of the ellipsoidal coordinates [*Tsyganenko,* 2000b].

The magnetopause magnetic field can be obtained using a straightforward numerical procedure, which minimizes the rms magnetic flux across the boundary by varying parameters of analytical potential fields, representing the effect of the Chapman-Ferraro currents inside the magnetosphere. That method was first suggested by *Schulz and McNab* [1987] and proved simple and fast tool for shielding all principal sources of the magnetospheric field [*Tsyganenko,* 1995, 1996; *Tsyganenko and Stern,* 1996].

The cross-tail current and Region 1 Birkeland current have a common feature that makes their global representation somewhat tricky. Namely, both currents intersect the magnetopause and close either on the boundary or in the magnetosheath. The actual path of their closure current cannot be determined on the basis of the internal magnetospheric measurements; moreover, even if it were known, no simple solution for the magnetic field could have been found: the only choice would be to resort to a numerical integration. Fortunately, there is no need to know the actual closure currents: given the boundary condition upon the total normal component B_n, it only suffices to correctly specify the current density $\mathbf{j}$ *inside* the magnetosphere in order to obtain a unique solution. The closure currents outside the magnetopause can, in fact, be defined in any arbitrary way: for example, we can extend the cross-tail current to infinity in the $\pm y$-direction, as was done in the T87 model [*Tsyganenko,* 1987], or close the current flow lines as circles (T96). This allows one to use simple analytical current sheets or disks [*Tsyganenko and Peredo,* 1994] and hence dramatically simplifies the model.

The third pillar, connecting the data with the mathematical frame of a model, requires algorithms that relate the strength and spatial configuration of individual field sources with the input parameters, including the state of the solar wind and IMF. It is relatively easy to define that relationship for the magnetopause source: the dominant parameter in that case is the solar wind pressure and, in a crude approximation, the magnetopause shrinks and expands self-similarly, with the scaling factor $[p/\langle p\rangle]^{\beta}$, where $\beta \sim 1/6$. In fact, the exact self-similarity does not hold, since the magnetopause shape also changes in response to the varying IMF; however, that effect is more difficult to replicate in the models, than the self-similar compression/expansion used in the T96 model.

Much less is known on the actual response of other current systems, especially of the Birkeland current systems and of the magnetotail. *Iijima and Potemra* [1982] correlated the densities of Region 1 Birkeland currents with a variety of interplanetary quantities and found that $\gamma = p^{1/2} B_t \sin(\theta/2)$ provided the highest correlation. The parameter γ was adopted in the T96 model for calibrating the overall strength of the Region 1 current, on a tacit assumption that the total current is roughly proportional to its density, as estimated by Iijima and Potemra. More specifically, the total current was assumed as a linear function of γ, whose slope and intercept, among other model parameters, were fitted by least squares to data.

The same parameter γ was used in a linear form, relating the strength of the cross-tail current and the solar wind state. That expression also included a term containing $\sqrt{p}$, since the ram pressure of the solar wind strongly affects the tail lobe field [e.g., *Fairfield and Jones,* 1996] and, hence, the cross-tail current.

The strength of the ring current in the T96 model was parameterized by a linear function of the Dst-index and $\sqrt{p}$. However, possible change of the ring current radius with growing Dst was neglected. As a result, the model overestimates the magnetic moment of the ring current (and hence its overall contribution to the total field) during major storms.

In spite of the limitations of its approach, large gaps and relatively low resolution of the data, the T96 model not only yields "visually reasonable" magnetospheric configurations, but also in many cases accurately predicts spatial/temporal variations of the field, obtained in independent observations. Figure 1 shows three magnetic field components, observed by POLAR on August 1, 1998. Not only the general features, but also fine details (e.g., between 9 and 19 UT) are reproduced fairly well. The agreement worsens towards the end of the day, after a disturbed period between 13 and 21 UT, and the model also misses a crossing of the field-aligned current between 4 and 5 UT. During that period the IMF was mostly northward and, hence, $\gamma \approx 0$. Due to the simple lin-

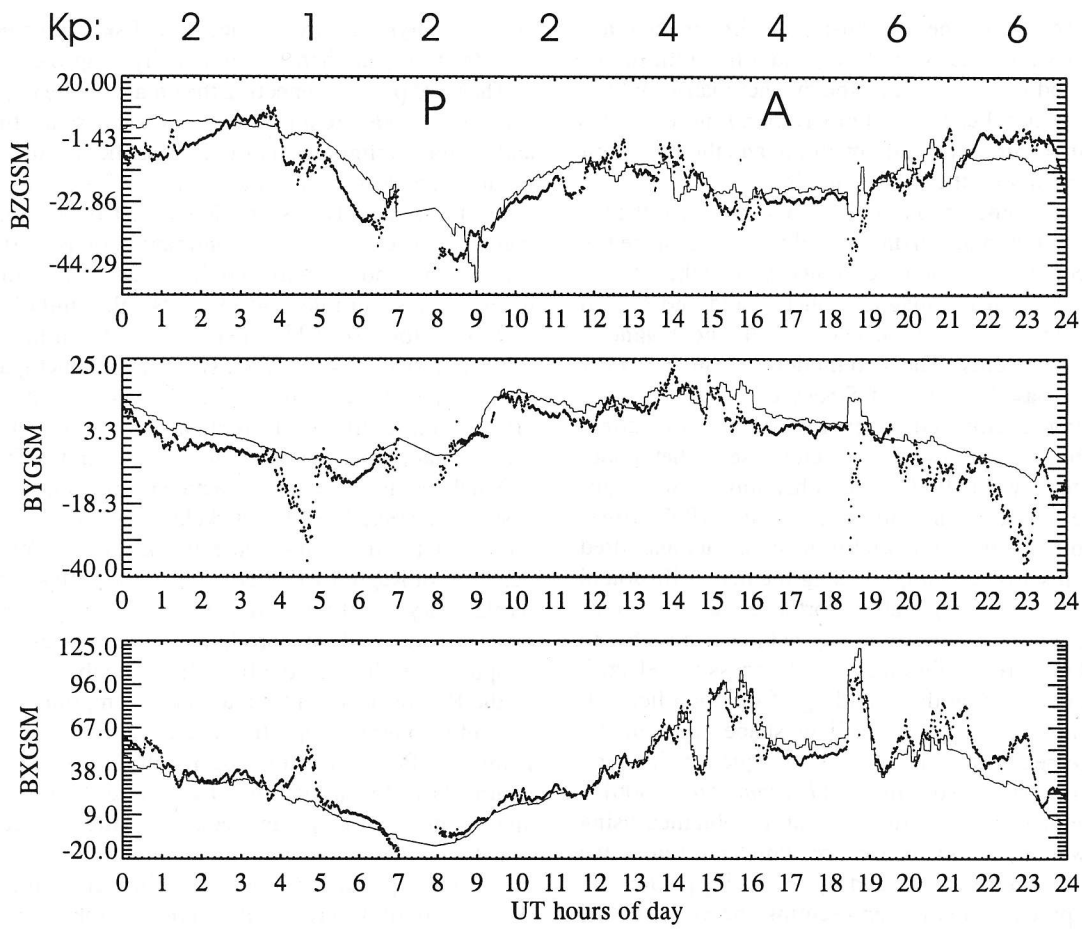

Figure 1. Comparison of the components of external field (geodipole contribution subtracted), observed by POLAR on 08/01/1998 (thick trace), with those predicted by the T96 model (thin trace). Kp-index values are shown above the plot. Letters P and A mark the times of Polar perigee and apogee, respectively.

ear parameterization of the Birkeland currents by γ, adopted in T96, their magnitude was grossly underestimated in the model. The generally insufficient magnitude of the model field-aligned currents, found in many instances, may be due to the virtual absence of the high-latitude observations in the modeling data set.

Figure 2 shows a similar plot, corresponding to an extremely disturbed day (August 27, 1998), with the Kp index ranging between 8 and 6. While the agreement in B_x component is quite good, in particular between 6 and 18 UT, the model grossly overestimates the depression in B_z inside the ring current. In this case, again, the discrepancy was caused by lack of data in the inner magnetosphere and an inflexible model ring current.

3. NEW FRONTIERS

As demonstrated above, efforts to further improve data-based magnetosphere models should address three principal areas: (i) rebuilding and extending the database, (ii) advanced mathematical representation of external field sources, and (iii) establishing optimal algorithms or relationships, quantifying the response of the magnetospheric currents to the solar wind input and/or the ground indices. In this section we concentrate on the last two aspects: how to improve a model's flexibility and how to best parameterize a model.

Magnetospheric currents have a complex and dynamic geometry. The magnetopause shrinks, expands, and erodes, with varying degrees of connection to the IMF. The tail current sheet warps, bends, and twists, in response to the geodipole wobbling and to the IMF. The tail current density undergoes dramatic redistribution as the tail stretches and rebounds. In addition, the substorms are accompanied by local disruptions of the tail current and its transient diversion into field-aligned currents. The injection of freshly accelerated particles into the inner magnetosphere results in formation of the storm-time ring current, while a significant part of the tail magnetic flux and plasma sheet particles are ejected tailward

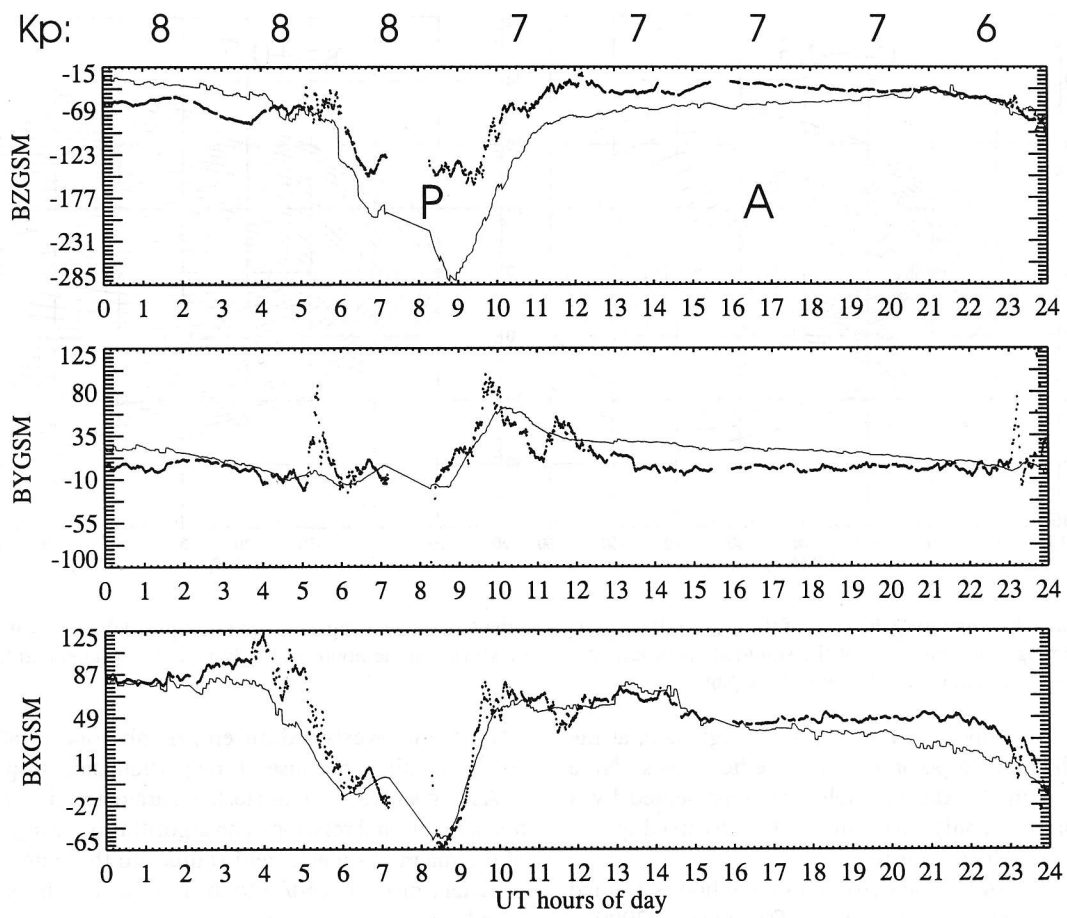

Figure 2. Same as in Figure 1, but for 08/27/1998.

as plasmoids. Large-scale Birkeland currents vary with the IMF and with the substorm cycle – and these are only average changes of the structure. To understand the physics (as well as to achieve concise models), the mathematical representations must resolve each of these variations in a meaningful way.

As recently demonstrated [*Tsyganenko,* 1998a], much flexibility can be added to the existing models by applying a divergence-conserving deformation of the magnetic field, whose basics were outlined by *Stern* [1987]. Using that approach, an economical method to warp and twist the tail current sheet was devised, consistent with the observed shapes of the plasma sheet and with the magnetopause response to the Earth's dipole tilt [*Tsyganenko et al.,* 1998]. Another simple deformation was suggested for the modeling of the structure of polar cusps, observed by POLAR [*Tsyganenko and Russell,* 1999].

In this paper, two other interesting uses of the deformation technique will be briefly described. The first one makes it possible to devise models with a variable profile of the cross-tail current density, in which the position of the inner edge of the current sheet and its tailward extent are controlled by a single parameter κ, and there is no need to recalculate the shielding currents. The essence of the method is to transform the shielded tail magnetic field vector $\mathbf{B}_T$ to the coordinates σ and τ, in which the T96 model magnetopause is specified as a surface $\sigma = \sigma_0$. In the front part of the magnetosphere ($\tau > 0$), σ and τ are the ellipsoidal coordinates [see *Tsyganenko,* 1989b, 1995, 2000b, for details], while in the rear part ($\tau < 0$) they convert to the cylindrical ones. Then we apply a simple stretch transformation $\tau \rightarrow \tau' = \tau'(\tau)$ and, since $\nabla\sigma \perp \nabla\tau$ and the coordinate σ remains intact, the deformation does not violate the shielding, so that the normal component of the deformed field remains zero. Figure 3 shows the lines of a shielded tail field in the noon-midnight meridian plane for two values of the stretch coefficient κ. The deformation conserves $\nabla \cdot \mathbf{B} = 0$, although it does not conserve $\nabla \times \mathbf{B}$, that is, gives rise to unphysical currents. In our case, however, owing to the smoothness of the transformation, the artificial current density remains relatively small even for large values of the stretch parameter. The above deformation can serve as a promising new tool for improving the accuracy of the

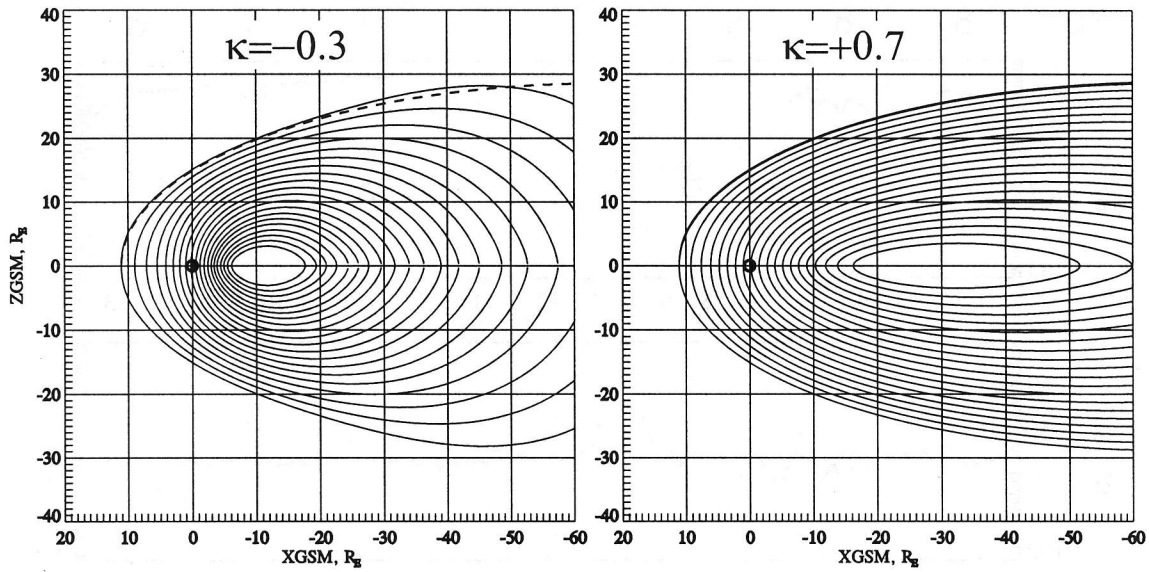

Figure 3. Illustrating the shift of the cross-tail current along the X-axis by using a stretch in ellipsoidal coordinates. The magnetic field lines of the shielded cross-tail current are shown in the noon-midnight meridian plane, and the electric current is directed out of the page.

models in a most important region on the nightside, at the interface of the quasi-dipolar and tail-like field lines. Note that in the T96 model the tail field was represented by a linear combination of only two terms, each with a fixed spatial distribution of the electric current.

In the second example the deformation method is applied to the field of a realistic ring current [*Tsyganenko,* 2000c]. In that work, a quantitative model was developed of the inner magnetospheric magnetic field, combining the effects of the azimuthally asymmetric ring current with those of field-aligned currents, caused by azimuthal variation of the plasma pressure. The axisymmetric part of the model ring current was derived from average profiles of the particle pressure and anisotropy, observed by AMPTE/CCE spacecraft, and was analytically represented by a vector potential, fitted by least squares to one derived by the Biot-Savart integral. The goal of the work was a realistic and computationally efficient global description of the ring current field, so it was important to obtain mathematically simple approximations. A solution for the axially symmetric part of the ring current was found as the field of a spread-out double current loop [*Tsyganenko,* 1998b], deformed in the space $\{\alpha, \gamma\}$ of orthogonal dipolar coordinates, where $\alpha = (x^2 + y^2)/r^3$ and $\gamma = z/r^3$. The difference between the model approximations and the original Biot-Savart field did not exceed a fraction of percent, with fairly simple analytical deformation functions $\alpha' = \alpha'(\alpha, \gamma)$ and $\gamma' = \gamma'(\alpha, \gamma)$. Further details are beyond the scope of this paper, but Figure 4 shows the lines of equal azimuthal current density in the model, in which a small region of the inner eastward current flows inside a much larger and radially extended westward current, visibly concentrated near the equatorial plane because of the particle anisotropy.

As said above, the main task in parameterizing a model is to find a functional relation or an algorithm, relating the strength of the magnetospheric field sources to the state of the interplanetary medium and/or to the routinely monitored ground-based (or magnetospheric) parameters, including their previous history. The parameterization assumed in the T96 model was by no means optimal, since the adopted relations were based mainly on simple a priori considerations, rather than on thorough correlation studies. That gap was partially bridged in our recent work [*Tsyganenko,* 2000a], in which a variety of functions was studied, describing the tail current response to

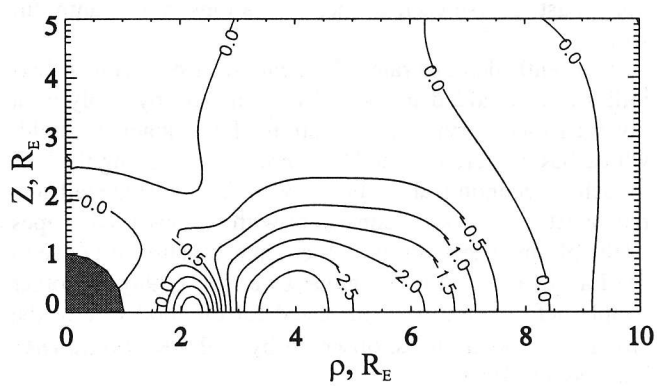

Figure 4. Distribution of the volume electric current density in the ring current model, based on the observed profiles of particle pressure and anisotropy [*Tsyganenko,* 2000c].

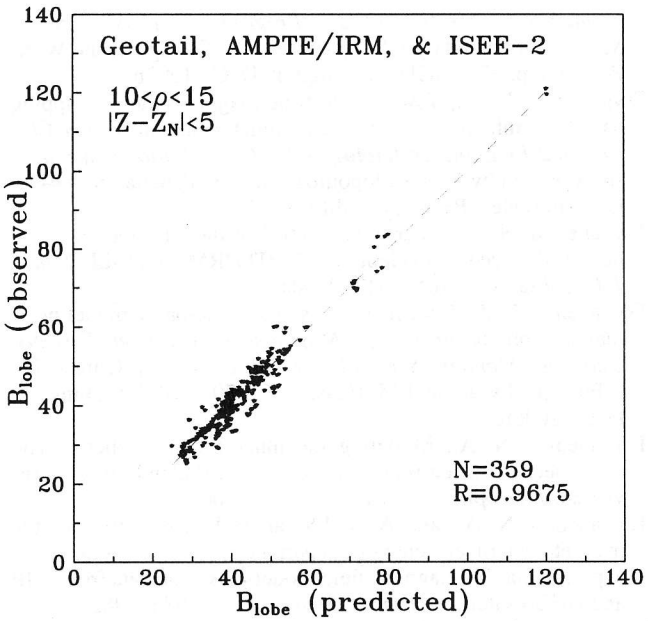

Figure 5. Scatter plot of the observed tail lobe field against that predicted by a linear regression relation, for $10 \leq \rho \leq 15$ [*Tsyganenko,* 2000a].

the solar wind state, and a linear filter technique was used to study the role of previous conditions on the current tail field strength. The study covered a wide range of tailward distance between 10 and 60 R_E and was based on a large set of tail lobe magnetic field data of Geotail (1993–97), AMPTE/IRM (1985–86), and ISEE-2 (1978–80). The tailward variation of the lobe field and its response to the solar wind and IMF conditions were studied using a regression relationship, including various combinations of the interplanetary quantities, measured by WIND and IMP 8. The regression relation included three terms, representing contributions from the Dst-index, solar wind ram pressure P_d, and IMF, using not only the concurrent values of the last two parameters, but also 12 previous values of their 5-min averages.

A detailed search was made for the best combination of the solar wind pressure- and IMF-related parameters, providing the highest value of the multiple correlation coefficient R between the predicted and observed lobe field. It was found that the near-tail field becomes significantly less sensitive to the solar wind pressure for large values of P_d, so that it is better described by a logarithmic law, rather than by a power law. Among various IMF-related regression functions, g, the best results for the near tail were obtained with $g = Vh(B_\perp)\sin^3(\theta/2)$, where the function h behaves as $B_\perp^2 = B_y^2 + B_z^2$ for commonly observed values of the IMF, but gradually transforms into a linear dependence for $B_\perp \geq 40nT$. The Dst term was found to yield a significant contribution to the regression relation in the nearest bin of the distance (10–15R_E), but its contribution rapidly fell off at larger distances. Overall, the optimal values of the regression coefficients yielded a very good fit in the near tail, especially in the nearest distance bin, where the correlation coefficient reached $R \approx 0.97$. Figure 5 shows the scatter plot of the observed against predicted values of the lobe field in the distance bin 10–15R_E.

With regard to the time lag effects, in the nearest interval of the distance the best fit linear filter function for the pressure-dependent term was found to rapidly increase with growing time lag, suggesting a significant average delay between the changes of the solar wind pressure and the reaction of the lobe field.

4. CONCLUDING COMMENTS

Significant progress has been made in the development of empirical magnetosphere field models. As shown here, even transient variations of the field components can be reproduced fairly accurately in many cases, even though the model is based on data from many periods in the past, with different interplanetary conditions. The recent accomplishments in the field of the modeling methods, as well as an ample inflow of the newly obtained data allow the development of new better models, which will advance the magnetic mapping of geospace. Future models will include a dynamical parameterization of the field sources, taking into account the effects of a time-delayed response. Finally, it is expected that the empirical modeling will play a crucial role in the future multi-spacecraft missions, making it possible to reconstruct instantaneous magnetospheric configurations from simultaneous field measurements at many different locations [*Tsyganenko,* 1998c].

Acknowledgments. I gratefully acknowledge David Stern for his many thoughtful comments on the manuscript. This work is supported by NASA grants NAS5-32350 and NAS5-32993, and NSF Magnetospheric Physics Program grant ATM-9819873.

REFERENCES

Campbell, W. H., Geomagnetic storms, the Dst ring-current myth and lognormal distribution, *J. Atmos. Terr. Phys., 58,* 1171, 1996.

Fairfield, D. H., N. A. Tsyganenko, A. V. Usmanov, M. V. Malkov, A large magnetosphere magnetic field database, *J. Geophys. Res., 99,* 11,319, 1994.

Fairfield, D. H., and J. Jones, Variability of the tail lobe field strength, *J. Geophys. Res., 101,* 7785, 1996.

Iijima, T., and T. A. Potemra, The relationship between interplanetary quantities and Birkeland current densities, *Geophys. Res. Lett., 9,* 442, 1982.

Mead, G.D., and D.H. Fairfield, A quantitative magnetospheric model derived from spacecraft magnetometer data, *J. Geophys. Res., 80,* 523, 1975.

Ostapenko, A. A., and Y. P. Maltsev, Relation of the magnetic

field in the magnetosphere to the geomagnetic and solar wind activity, *J. Geophys. Res., 102,* 17,467, 1997.

Peredo, M., D. P. Stern, and N. A. Tsyganenko, Are existing magnetospheric models excessively stretched ?, *J. Geophys. Res., 980,* 15,343, 1993.

Schulz, M., and M. McNab, Source-surface model of the magnetosphere, *Geophys. Res. Lett., 14,* 182, 1987.

Shue, J.-H., J. K. Chao, H. C. Fu, C. T. Russell, P. Song, K. K. Khurana, and H. J. Singer, A new functional form to study the solar wind control of the magnetopause size and shape, *J. Geophys. Res., 102,* 9497, 1997.

Shue, J.-H., P. Song, C. T. Russell, J. T. Steinberg, J. K. Chao, G. Zastenker, O. L. Vaisberg, S. Kokubun, H. J. Singer, T. R. Detman, and H. Kawano, Magnetopause location under extreme solar wind conditions, *J. Geophys. Res., 103,* 17,691, 1998.

Sibeck, D. G., R. E. Lopez, and E. C. Roelof, Solar wind control of the magnetopause shape, location, and motion, *J. Geophys. Res., 96,* 5489, 1991.

Stern, D. P., Tail modeling in a stretched magnetosphere, 1, Methods and transformations, *J. Geophys. Res., 92,* 4437, 1987.

Tsyganenko, N. A., Global quantitative models of the geomagnetic field in the cislunar magnetosphere for different disturbance levels, *Planet. Space Sci., 35,* 1347, 1987.

Tsyganenko, N. A., A magnetospheric magnetic field model with a warped tail current sheet, *Planet. Space Sci., 37,* 5, 1989a.

Tsyganenko, N.A., A solution of the Chapman-Ferraro problem for an ellipsoidal magnetopause, *Planet.Space Sci., 37,* 1037, 1989b.

Tsyganenko, N. A., Modeling the Earth's magnetospheric magnetic field confined within a realistic magnetopause, *J. Geophys. Res., 100,* 5599, 1995.

Tsyganenko, N. A., Effects of the solar wind conditions on the global magnetospheric configuration as deduced from data-based field models, *Eur. Space Agency Spec. Publ., ESA SP-389,* 181, 1996.

Tsyganenko, N. A., Modeling of twisted/warped magnetospheric configurations using the general deformation method, *J. Geophys. Res., 103,* 23551, 1998a.

Tsyganenko, N. A., Data-based models of the global geospace magnetic field: Challenges and prospects of the ISTP era, in *Geospace Mass and Energy Flow: Results From the International Solar-Terrestrial Physics Program, Geophys. Monogr. Ser., v. 104,* edited by J. L. Horwitz, D. L. Gallagher, and W. K. Peterson, p. 371, AGU, Washington, D. C., 1998b.

Tsyganenko, N. A., Toward real-time magnetospheric mapping based on multi-probe space magnetometer data, in *Science Closure and Enabling Technologies for Constellation Class Missions*, edited by V. Angelopoulos and P. V. Panetta, pp. 84-90, U. C. Berkeley, Berkeley, California, 1998c.

Tsyganenko, N. A., Solar wind control of the tail lobe magnetic field as deduced from Geotail, AMPTE/IRM, and ISEE 2 data, *J. Geophys. Res., 105,* 5517, 2000a.

Tsyganenko, N. A., Recent progress in the data-based modeling of magnetospheric currents, in: *Magnetospheric Current Systems, Geophys. Monogr. Ser., vol. 118,* edited by S.-I. Ohtani, R.-I. Fujii, R. Lysak, and M. Hesse, p.61–70, AGU, Washington, D. C., 2000b.

Tsyganenko, N. A., Modeling the inner magnetosphere: The asymmetric ring current and region 2 Birkeland currents revisited, *J. Geophys. Res., 105,* in press, 2000c.

Tsyganenko, N. A., and A. V. Usmanov, Determination of the magnetospheric current system parameters and development of experimental geomagnetic field models based on data from IMP and HEOS satellites, *Planet. Space Sci., 30,* 985, 1982.

Tsyganenko, N. A., and M. Peredo, Analytical models of the magnetic field of disk-shaped current sheets, *J. Geophys. Res., , 99,* 199, 1994.

Tsyganenko, N. A., and Stern, D. P., Modeling the global magnetic field of the large-scale Birkeland current systems, *J. Geophys. Res., 101,* 27,187, 1996.

Tsyganenko, N. A. and C. T. Russell, Magnetic signatures of the distant polar cusps: Observations by Polar and quantitative modeling, *J. Geophys. Res., 104,* 24,939, 1999.

Tsyganenko, N. A., S. B. P. Karlsson, S. Kokubun, T. Yamamoto, A. J. Lazarus, K. W. Ogilvie, C. T. Russell, Global configuration of the magnetotail current sheet as derived from Geotail, Wind, IMP 8 and ISEE 1/2 data, *J. Geophys. Res., 103,* 6827, 1998.

N. A. Tsyganenko, Raytheon ITSS/Code 690.2, NASA Goddard SFC, Greenbelt, MD 20771. (e-mail: ys2nt@lepvx3.gsfc.nasa.gov)